

Angular Dependences of Perpendicular and Parallel Mode Electron Paramagnetic Resonance of Oxidized Beef Heart Cytochrome *c* Oxidase

Dominic J. B. Hunter,* Vasily S. Oganessian,[‡] John C. Salerno,[‡] Clive S. Butler,[†] W. John Ingledew,* and Andrew J. Thomson[‡]

*School of Biological and Medical Sciences, University of St. Andrews, St. Andrews, Fife KY16 9AL, Scotland; [†]Department of Biology, Rensselaer Polytechnic Institute, Troy, New York 12180 USA; and [‡]Centre for Metalloprotein Spectroscopy and Biology, School of Biological Sciences and School of Chemical Sciences, University of East Anglia, Norwich, Norfolk NR4 7TJ, UK

ABSTRACT Cytochrome *c* oxidase catalyzes the reduction of oxygen to water with a concomitant conservation of energy in the form of a transmembrane proton gradient. The enzyme has a catalytic site consisting of a binuclear center of a copper ion and a heme group. The spectroscopic parameters of this center are unusual. The origin of broad electron paramagnetic resonance (EPR) signals in the oxidized state at rather low resonant field, the so-called $g' = 12$ signal, has been a matter of debate for over 30 years. We have studied the angular dependence of this resonance in both parallel and perpendicular mode X-band EPR in oriented multilayers containing cytochrome *c* oxidase to resolve the assignment. The “slow” form and compounds formed by the addition of formate and fluoride to the oxidized enzyme display these resonances, which result from transitions between states of an integer-spin multiplet arising from magnetic exchange coupling between the five unpaired electrons of high spin Fe(III) heme a_3 and the single unpaired electron of Cu_B . The first successful simulation of similar signals observed in both perpendicular and parallel mode X-band EPR spectra in frozen aqueous solution of the fluoride compound of the closely related enzyme, quinol oxidase or cytochrome bo_3 , has been reported recently (Oganessian et al., 1998, *J. Am. Chem. Soc.* 120:4232–4233). This suggested that the exchange interaction between the two metal ions of the binuclear center is very weak ($|J| \approx 1 \text{ cm}^{-1}$), with the axial zero-field splitting ($D \approx 5 \text{ cm}^{-1}$) of the high-spin heme dominating the form of the ground state. We show that this model accounts well for the angular dependences of the X-band EPR spectra in both perpendicular and parallel modes of oriented multilayers of cytochrome *c* oxidase derivatives and that the experimental results are inconsistent with earlier schemes that use exchange coupling parameters of several hundred wavenumbers.

INTRODUCTION

Mitochondrial cytochrome *c* oxidase (ferrocytochrome *c*: oxygen oxidoreductase, EC 1.9.3.1) catalyzes the reduction of oxygen to water and couples the free energy of this reaction with the extrusion of protons from the mitochondrial matrix. Extensive analysis of this enzyme, using a wide variety of techniques, has revealed much about its structure and function, but the recent publication of the crystal structures of bovine cytochrome *c* oxidase (Tsukihara et al., 1995, 1996) and *Paracoccus denitrificans* cytochrome *c* oxidase (Iwata et al., 1995), a bacterial homolog of the mammalian enzyme, has placed mechanistic studies on a more secure basis. The enzyme has four redox-active metal centers Cu_A , heme *a*, heme a_3 , and Cu_B . Cu_A , a binuclear copper site, transfers electrons via low-spin, six-coordinate heme *a*, liganded by two histidine groups, to the binuclear catalytic center. The catalytic center comprises a high-spin, five-coordinate heme a_3 and Cu_B , bound to three histidine ligands. This is the site of oxygen binding and

reduction and, possibly, of the process of proton translocation. The site is energy conserving and, by a mechanism that is still unclear, couples the energy to proton translocation. The protein structure was modeled with surprising accuracy before the resolution of the crystal structure, by a combination of site-directed mutagenesis, sequence comparisons, and various biophysical methods (Hosler et al., 1993; Brown et al., 1994). All of the redox active metal centers lie in one of two subunits. The Cu_A site is bound by subunit II, the remaining centers by subunit I. Hemes *a* and a_3 lie on opposite sides of transmembrane helix X, at an angle of 104° to each other but with both heme planes perpendicular to the membrane. Heme *a* is ligated by His⁶¹ from helix II and His³⁷⁸ from helix X and heme a_3 by His³⁷⁶ of helix X (bovine numbering). Cu_B lies close to the high-spin heme a_3 , coordinated by His²⁴⁰, from helix VI, and His²⁹⁰ and His²⁹¹ from helices VII and VIII (Tsukihara et al., 1995; Iwata et al., 1995).

Electron paramagnetic resonance (EPR) spectroscopy has been an important biophysical tool for the study of the individual metal sites of this complex enzyme. At X-band in the oxidized state, all forms of the enzyme show a rhombic trio of signals, $g_z = 3.0$, $g_y = 2.25$, and $g_x = 1.45$, arising from low-spin Fe(III) heme *a* and a rather broad signal, lacking well-resolved metal hyperfine structure, around $g = 2$ arising from Cu_A (Lappalainen and Saraste, 1994). A weak signal observed at $g_{xy} = 6$ comes from high-spin Fe(III) heme and is probably due to reduction of a small

Received for publication 16 March 1999 and in final form 9 September 1999.

Dr. Hunter and Dr. Oganessian contributed equally to this paper.

Address reprint requests to Dr. Andrew J. Thomson, University of East Anglia, School of Chemical Sciences, Norwich NR4 7TJ, U.K. Tel.: 44-1603-592023; Fax: 44-1603-592710; E-mail: a.thomson@uea.ac.uk.

© 2000 by the Biophysical Society

0006-3495/00/01/439/12 \$2.00

amount of Cu_B to the diamagnetic state or to a small amount of enzyme lacking Cu_B (Hunter et al., 1997). The heme a_3 - Cu_B binuclear center gives rise, under certain conditions, to highly unusual EPR signals, depending on the history of the enzyme. Because this site has been difficult to probe by optical and magnetic techniques, these signals have been of great interest. However, their assignment and interpretation are still controversial.

Cytochrome *c* oxidase may be isolated in a number of forms. Of interest here are the "slow" form of the enzyme and compounds formed by the addition of formate and fluoride. These all display unusual low-field EPR resonances, which are believed to arise from transitions between states of an integer-spin multiplet that result from the magnetic coupling between the five unpaired electrons of heme a_3 and the single unpaired electron on Cu_B . As usually prepared, the "slow" form of the enzyme shows a slow rate of internal electron transfer, sluggish ligand binding, and a broad EPR resonance at $g' = 12$ (Brudvig et al., 1981; Schoonover and Palmer, 1990; Cooper and Salerno, 1992). Cycling the enzyme with reductant in the presence of oxygen generates a so-called fast form of the enzyme with a fast internal electron transfer between hemes *a* and a_3 and rapid ligand binding. The EPR resonance at $g' = 12$ is absent from this form of the enzyme. A "fast" to "slow" conversion can be achieved by incubation of the enzyme at low pH or by treatment with formate (Schoonover and Palmer, 1990). These treatments restore the $g' = 12$ resonance, typical of the integer-spin complexes of cytochrome *c* oxidase. A weak resonance at $g' = 2.95$ is always present with the $g' = 12$ signal and shows temperature and power saturation dependences similar to those of the $g' = 12$ signal. This must also arise from the same integer-spin species. Binding of fluoride to cytochrome *c* oxidase gives rise to a complex series of resonances at $g' = 8.5, 6, 5, 4.3$, and 3.2 , the signals at $g = 6$ and $g = 4.3$ coming from uncoupled high-spin ferric heme and from low-symmetry nonheme iron (Cooper and Salerno, 1992).

A comparison between the EPR signals found in the bacterial quinol oxidase, cytochrome bo_3 , and cytochrome *c* oxidase is instructive. Spectroscopic studies and close sequence homologies show these oxidases to be closely related (Chepuri and Gennis, 1990), although Cu_A is absent from subunit II of cytochrome bo_3 , presumably because this enzyme accepts electrons from quinol rather than cytochrome *c*. In oxidized cytochrome bo_3 , a variety of ligands, including F^- , HCOO^- , and H_2O , bind heme o_3 , which remains high-spin Fe(III), $S = 5/2$ (Cheesman et al., 1994; Ingledew et al., 1993; Calhoun et al., 1994; Little et al., 1996). Perpendicular mode X-band EPR spectra of all these derivatives show broad, fast relaxing features with the overall pattern of a weak derivative signal at $g' \approx 12$ region accompanied by a broad band in the region of $g' \approx 3.2$ (Watmough et al., 1993). In the parallel mode X-band

spectrum only the low-field signal is present. Hence these signals are very similar to those reported for the slow and various inhibited forms of bovine cytochrome *c* oxidase (Greenaway et al., 1977; Hagen, 1982) and attest to a close structural relationship between the active sites in the two enzymes.

The orientation of heme *a* of cytochrome *c* oxidase was first established by measurements of the angular dependence of the EPR signals of the enzyme in oriented multilayers of mitochondrial membranes (Blum et al., 1978). The crystal structures of cytochrome *c* oxidase confirm the heme orientation deduced from these studies. Heme *a* lies with its normal in the membrane plane, the g_x and g_y signals being at 60° and 30° to the membrane, respectively (Blum et al., 1978). The hemes of cytochrome bo_3 have a similar orientation (Salerno and Ingledew, 1991). The EPR resonances of heme *a* correspond to the in-heme-plane projections of the d_{xz} and d_{yx} orbitals and so approximate to the axes of highest and lowest unpaired electron density. The angular dependence of the minor species of high-spin ferric heme signal at $g = 6$ showed that heme a_3 is also oriented with its normal in the membrane plane.

The orientation dependence of the X-band EPR signals in both perpendicular and parallel modes, displayed by these integer-spin complexes, is addressed in this paper. The aim is to assess the validity of theoretical models describing the interaction between the heme-copper pair. Additional orientation-dependent experiments are reported with the EPR spectrometer operating in parallel mode, that is, with the applied magnetic field (\mathbf{B}_0) and the magnetic field of the incident microwave radiation (\mathbf{B}_1) parallel to one another. This contrasts with the more usual perpendicular mode measurements in which \mathbf{B}_0 is applied perpendicular to the applied magnetic field. The advantage of making this comparison is that the selection rules for magnetic dipole microwave transitions are different in the two modes and hence are complementary to one another.

Recently, the first successful simulation of both perpendicular and parallel mode X-band EPR spectra of fluoride- bo_3 has been reported (Oganesyan et al., 1998). This reveals that there is only a very weak exchange interaction ($|\mathbf{J}| \approx 1 \text{ cm}^{-1}$) between the two metal ions of the binuclear center and shows that, in species exhibiting these broad signals, the presence of ligands bound either to heme a_3 or to Cu_B play only a minor part in mediating the interaction between a_3 and Cu_B . We show here that this model accounts well for the angular dependences of the X-band EPR spectra of cytochrome *c* oxidase derivatives in both perpendicular and parallel modes and, indeed, further shows that the experimental results are not consistent with earlier schemes that use exchange coupling parameters of several hundred cm^{-1} . The results give strong support to the proposed weak coupling scheme (Oganesyan et al., 1998).

MATERIALS AND METHODS

Preparation of mitochondrial membranes

Mitochondria (heavy mitochondrial fraction) were prepared from ox heart muscle (Green and Ziegler, 1963) and were disrupted by a single passage through a French pressure cell as described previously (Salerno and Ingledew, 1991).

Oriented multilayers

Mitochondrial membrane fragments, suspended to ~15 mg protein/ml in 2 mM HEPES (pH 7.4), were immediately used for multilayer preparation or were incubated with 10 mM sodium fluoride or sodium formate in the above buffer for 24 h on ice. Oriented multilayers were then prepared by depositing the treated mitochondrial membranes onto a nitrocellulose-coated acetate sheet by centrifugation in a swinging bucket rotor (Beckman SW28) at $50,000 \times g$ for 1 h at 4°C (Blum et al., 1978). Hemispherical polycarbonate inserts were used to produce a flat internal bottom to the centrifuge tube. The deposited membranes were dried under a gentle stream of nitrogen for 1–3 h before being sliced into strips and inserted into quartz EPR tubes of ~3 mm internal diameter. The EPR tubes were then quickly frozen and stored under liquid nitrogen until use.

Electron paramagnetic resonance spectroscopy

Perpendicular mode EPR spectra were obtained using a Bruker ER200D spectrometer interfaced to a ESP3220 computer (Bruker Analytische Messtechnik GmbH, Silberstreifen, W-7512, Rheinstetten 4, Germany) equipped with a variable-temperature cryostat and liquid helium transfer line (Oxford Instruments, Osney Mead, Oxford, England). Parallel mode EPR spectra were obtained using a Bruker ER300D spectrometer fitted with a dual mode cavity, (type ER4116DM), which can be switched between modes by tuning at different frequencies. In these experiments perpendicular mode spectra were obtained at 9.67 GHz, while parallel mode spectra were obtained at 9.37 GHz. The angle between the plane of the sample sheet and the applied magnetic field was measured with a goniometer. The angle between the plane of the sample (and thus the membrane) and the applied magnetic field is defined as θ , such that $\theta = 0^\circ$ when the field lies in the plane and $\theta = 90^\circ$ when the field is normal to the plane.

RESULTS

Perpendicular mode EPR spectroscopy

Perpendicular mode X-band EPR spectra of oxidized ("slow") fluoride- and formate-treated mitochondrial membranes, recorded with the applied magnetic field (B_0) at various angles between -15° and 105° to the plane of the membranes, are shown in Figs. 1, 2, and 3, respectively. The signal at $g = 6$ is the $g_{x,y}$ resonance of magnetically isolated high-spin Fe(III) heme a_3 , and the peak at $g = 3.0$ is the g_z resonance of low-spin Fe(III) heme a . The angular variation of these two signals allows the orientation of the membrane to be established and provides a measure of the mosaic spread of individual protein molecules. Previous work (Blum et al., 1978) on the EPR of oriented layers showed that the low-spin heme a plane contains the normal to the membrane. This result is confirmed by recent crystal structures, which also show that heme a_3 has a similar orientation

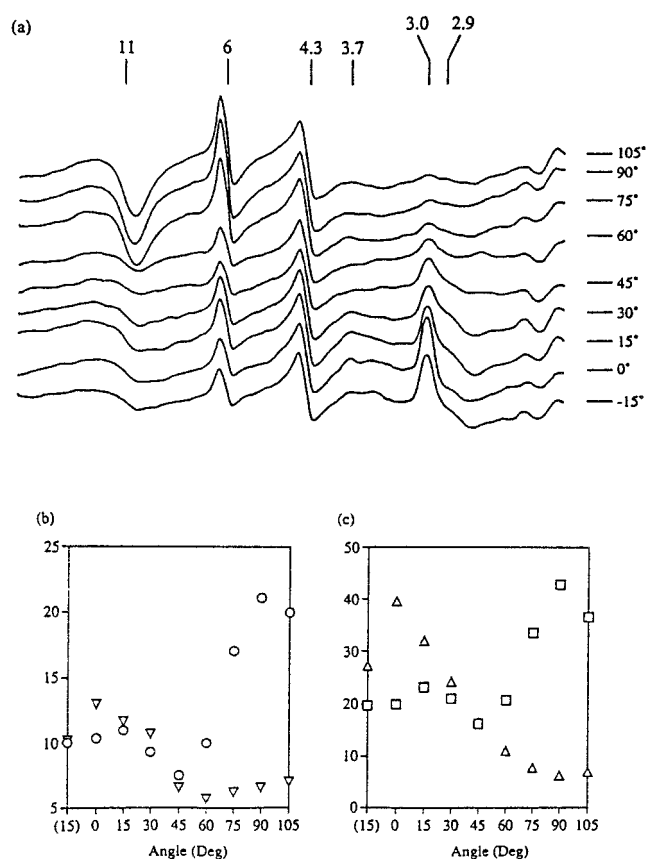


FIGURE 1 (a) EPR spectra of oriented multilayers prepared from mitochondrial membranes containing untreated, oxidized ("slow") cytochrome *c* oxidase, recorded with the applied magnetic field at angles (θ) between -15° and 105° to the plane of the multilayers. The g values of the major resonances are shown above the spectra. (b and c). Variation of the intensities with angle of applied magnetic field to membrane plane: $g = 12$ (\circ), $g = 6$ (\square), $g = 3.7$ (∇), $g = 3$ (\triangle). EPR spectrometer settings: modulation amplitude 4 G, microwave power 20 mW, frequency 9.45 GHz, temperature 4–5 K.

with respect to the membrane plane. Therefore the signals from the two hemes are expected to have opposite polarizations, with $g_{xy} = 6$ being at maximum when the membrane normal is parallel to the applied magnetic field. The signal at $g_z = 3$, arising from the low-spin ferric heme, will be at maximum with the applied magnetic field parallel to the membrane plane. The $g_y = 2.25$ resonance from the low-spin ferric heme was largely obscured in these samples by strong overlapping resonances from other components in the membranes. As well as these angular dependent resonances, the spectrum of rhombic high-spin $S = 5/2$ adventitious Fe(III) was observed at $g = 4.3$. This arises from an isotropic Kramers doublet and hence shows no orientation dependence. In addition, signals arising from the $\text{Cu}_B(\text{II})$ - $\text{Fe}_{a_3}(\text{III})$ coupled pair are observed. Since the g values arising from such systems will in general depend on the microwave frequency used, they are labeled as effective g values (g') (Brudvig et al., 1980).

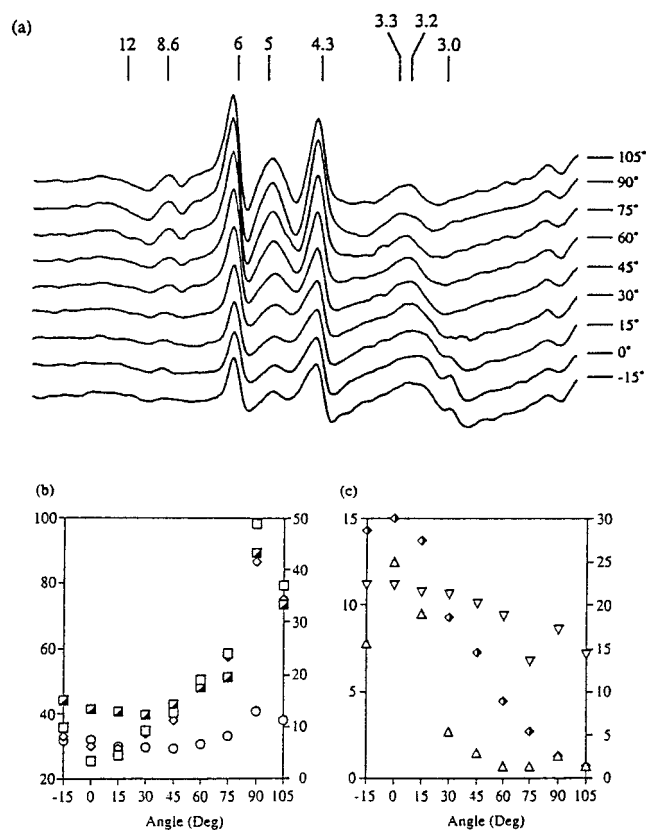


FIGURE 2 (a) EPR spectra of oriented multilayers prepared from mitochondrial membranes containing cytochrome *c* oxidase treated with 10 mM sodium fluoride for 24 h before multilayer production. (b and c) Variation of the intensities of resonances with angle of applied magnetic field: $g = 12$ (○), $g = 6$ (□), $g = 5$ (◇), $g = 4.3$ (■), $g = 3.3/3.2$ (▽), $g = 3$ (△), $g = 3.15$ (◄) (difference, measurement at X° subtracted from that at 0°). Spectrometer conditions were as for Fig. 1.

The EPR spectra of “slow” cytochrome *c* oxidase (Fig. 1*a*), with the applied magnetic field at -15° to 105° to the plane of the multilayers, gives signals at $g' = 11$, 3.7, and 2.9 in addition to those at $g = 6$ and $g_z = 3$. Similar signals have been reported at $g' = 12$ and $g' = 2.95$ (Cooper and Salerno, 1992). The variations in intensity with orientation are given graphically in Fig. 1, *b* and *c*, showing that the $g' = 11$ resonance is at maximum with the applied magnetic field perpendicular to the multilayer plane ($\theta = 90^\circ$). Other resonances are less clearly defined because of their low intensity. The $g' = 3.7$ signal appears to be at maximum with the applied magnetic field parallel to the plane of the multilayers ($\theta = 0^\circ$). The $g' = 2.9$ resonance is partially obscured by the $g_z = 3$ resonance of the low-spin ferric heme but appears to be at maximum with the field at around 30° to the multilayers.

The spectra of the fluoride-treated oxidase are shown in Fig. 2*a*. Resonances at $g = 8.6$, 6, 5, 4.3 and a broad peak between 3.3 and 3.2 and 3.0 are prominent, comparing well with those of the published spectrum of unoriented samples

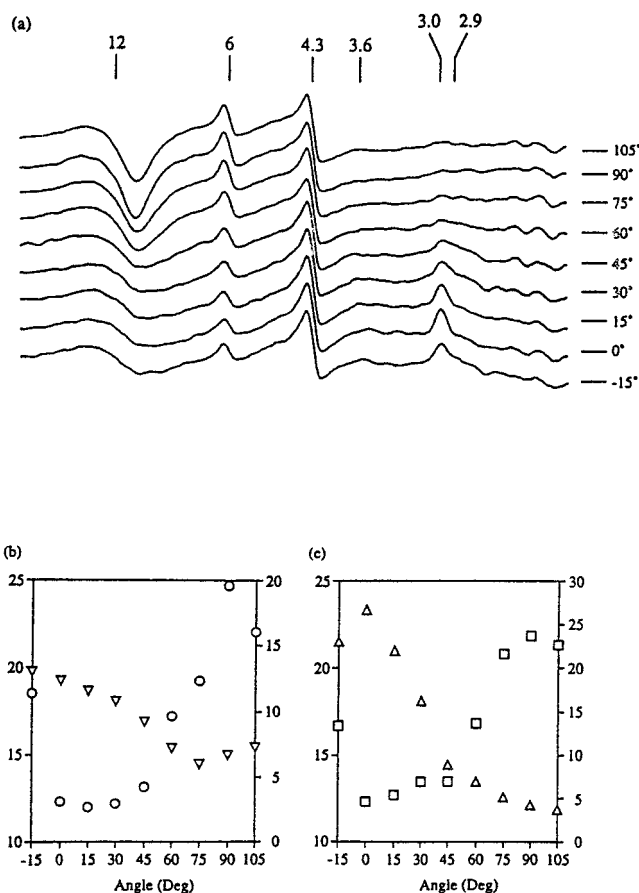


FIGURE 3 (a) EPR spectra of oriented multilayers prepared from mitochondrial membranes containing cytochrome *c* oxidase treated with 10 mM sodium formate for 24 h before multilayer production. (b and c) Variation of the intensities of resonances with angle of applied magnetic field: $g = 12$ (○), $g = 6$ (□), $g = 3.6$ (▽), $g = 3$ (△). Spectrometer conditions were as for Fig. 1.

(Schoonover and Palmer, 1990). The resonances at $g = 6$ and $g = 4.3$ overlay the positions of existing resonances from high-spin ferric heme and low-symmetry nonheme iron: a comparison of Fig. 2*a* with Figs. 1*a* and 3*a* shows this clearly. In addition, resonances at $g' = 12$ and at $g_z = 3$ are visible. The latter resonance, arising from the low-spin ferric heme, is oriented as described previously (Blum et al., 1978). Again, the $g = 2.25$ resonance was obscured.

Fig. 2, *b* and *c*, plots the angular dependence of the resonances of fluoride-treated oxidase at $g = 12$, 8.6, 6, 5, 3.3/3.2, and 3. All except that at $g = 3.3/3.2$ show a marked angular dependence. The $g = 12$, 8.6, 6, 5 resonances are at maximum with the applied magnetic field perpendicular to the plane of the multilayers ($\theta = 90^\circ$). The $g = 3.3/3.2$ resonance is broad, with an ill-defined peak g value that decreases somewhat in magnitude as the angle of the applied magnetic field to the multilayer plane increases from 0° to 90° , but the main change is a narrowing of the peak width as this angle increases.

Fig. 3 *a* shows the orientation dependence of the EPR spectra of the formate compound of cytochrome *c* oxidase, and Fig. 3, *b* and *c*, plots the angular dependences of the intensities. The spectra are similar to those of the unligated, oxidized oxidase, with resonances at $g = 12, 6, 4.3, 3.6, 3$, and 2.9 . The angular variation of the $g = 6$ and $g = 3$ resonances indicate the degree of orientation and the extent of mosaic spread. The intensity maxima for the $g' = 12$ resonance occur with the applied field perpendicular, $\theta = 90^\circ$, for the $g = 3.6$ signal with the field parallel, $\theta = 0^\circ$ and for the $g' = 2.9$ resonance with the field at 30° to the membrane plane, $\theta = 30^\circ$.

Parallel mode EPR spectroscopy

Parallel mode EPR spectra of the unligated, oxidized cytochrome *c* oxidase and of fluoride-cytochrome *c* oxidase as a function of orientation are shown in Fig. 4. The parallel mode spectra of the formate compound (not shown) were virtually identical to those of the unligated, oxidized cytochrome *c* oxidase. All of the spectra are featureless at fields above $g = 6$, except for an orientation independent step feature at around $g = 4$ (not shown). The parallel mode signal at $g' = 10.3$ of oxidized, unligated oxidase shows a broad trough of maximum depth with the magnetic field perpendicular to the membrane plane ($\theta = 90^\circ$), whereas the spectra of the fluoride form gives two troughs, at $g' = 10.7$ and 8.0 , with similar orientations.

ANALYSIS OF RESULTS

The results show that the low field signals in both perpendicular and parallel modes have their maximum values when the applied magnetic field lies in the heme plane and are at minimum when the field is along the heme normal. Although the spectra of the “slow” and formate-treated enzyme have very similar spectral shapes and angular dependences in the perpendicular mode, the low field region is somewhat more complex in the fluoride-treated form. In the following sections we present an analysis of the angular dependence of the low field signal that reproduces the main features of the observed signals of oriented multilayers, namely, the angular variation of their intensities and shapes. We do not attempt to fit the spectra because the computer time required for such a process would be considerable. The need to vary parameters, including linewidths, would make the task unmanageable.

Coordinate system

The coordinate systems used for analysis of the experiments are shown in Fig. 5. *XYZ* and *xyz* define the membrane and heme coordinate systems, respectively, with *XY* defining the membrane plane and *xy* lying in the *YZ* plane, so that the

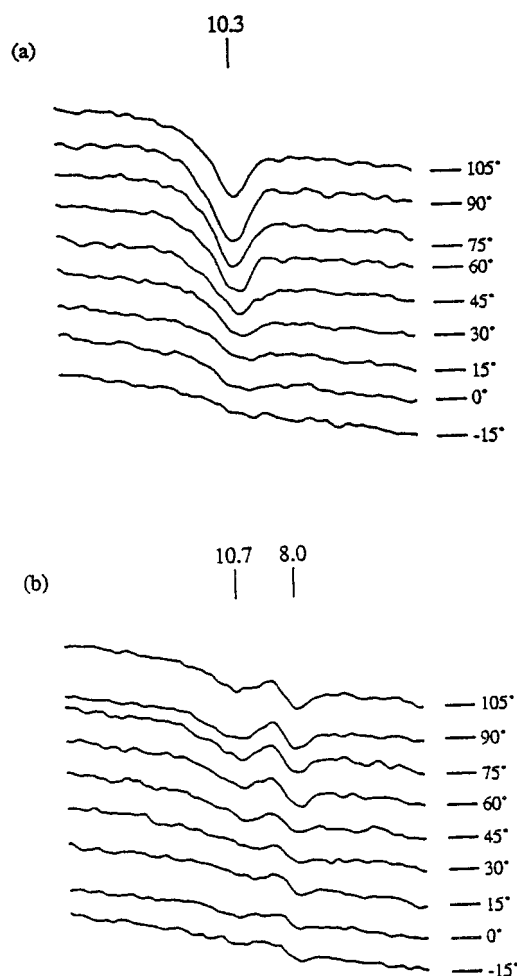


FIGURE 4 Parallel mode EPR spectra of (a) untreated, oxidized (“slow”) cytochrome *c* oxidase and (b) cytochrome *c* oxidase treated with sodium fluoride as described in the legend to Fig. 2. Spectra were recorded with the applied magnetic field at angles θ between -15° and 105° to the plane of the multilayers. The effective g values of the major features are shown above the spectra. EPR spectrometer settings: modulation amplitude 4 G, microwave power 20 mW, frequency 9.37 GHz, temperature 4–5 K.

orientation of the heme normal, z , is in the *XY*, that is, the membrane plane. The angle α describes the orientation of the heme *xy* axes relative to the membrane normal, Z . Because the *x* and *y* axes are equivalent for high-spin Fe(III) heme, this angle is unimportant for calculations of its EPR spectra. However, for a binuclear coupled system this angle is of crucial importance for the simulation of EPR line-shapes and intensities because the presence of a nonzero rhombicity $E \neq 0$ ensures the *x* and *y* axes are inequivalent. The direction of the applied magnetic field \mathbf{B}_0 is defined by two angles θ, ϕ , whereas \mathbf{B}_1 , the oscillating microwave magnetic field, is always in the *XY* plane. For each particular orientation of the applied magnetic field relative to the membrane plane, the random distribution of heme normals in the membrane plane and the presence of mosaic spread

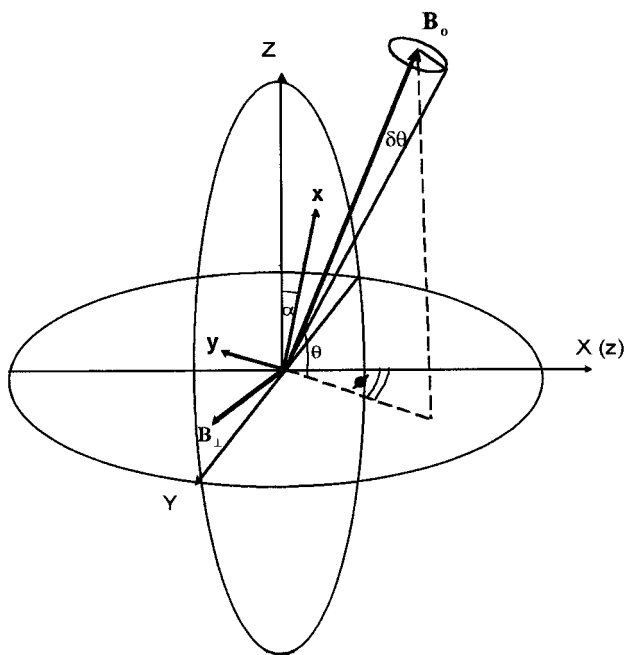


FIGURE 5 XYZ and xyz are the membrane and heme coordinate frames, where Z and z are the normals to the membrane and heme planes, respectively. YZ lies in the xy plane. The angle α measures the orientation of the heme xy axes relative to the membrane normal, Z . The direction of the applied magnetic field \mathbf{B}_0 is defined by two angles θ , ϕ , whereas \mathbf{B}_\perp and \mathbf{B}_\parallel , the oscillating microwave magnetic fields, are always either fixed in the XY plane or parallel to \mathbf{B}_0 , respectively. The cone of half-angle $\delta\theta$ defines the mosaic spread.

(see later) require averaging between $0 \leq \phi \leq 360^\circ$ and $0 \leq \theta \leq 180^\circ$ with a weighting factor $Q(\theta - \theta_0)$.

EPR simulation method

A general computer program for the simulation of EPR spectra, developed by one of us (VSO), has been adapted for the simulation of the EPR spectra of oriented multilayers including cases of non-Kramers systems. The following general expression is used (van Veen, 1978):

$$I_{\perp(\parallel)}(B) = \frac{1}{N(\theta_0, \sigma_\theta)} \sum_{i,j} \int_0^\pi \int_0^{2\pi} \left| \frac{\partial B_{ij}^r}{\partial h\nu} \right| \cdot \langle M_{ij}(\perp(\parallel)) \rangle P(B - B_{ij}^r) n_{ij}(T) Q(\theta - \theta_0) \sin \theta \, d\theta \, d\phi \quad (1)$$

B_{ij}^r is the field position for resonance between states i and j , and $\langle M_{ij}(\perp(\parallel)) \rangle$ represents the transition probability of absorption of microwave radiation of energy $h\nu$ between these states in either parallel or perpendicular mode. The experimental conditions constrain the microwave field B_\perp to lie in the membrane plane. $P(B - B_{ij}^r)$ is a normalized lineshape function of field, and the factor $|\partial B_{ij}^r / \partial h\nu|$ converts frequency-swept to field-swept spectra as described elsewhere (Hendrich and Debrunner, 1989; van Veen, 1978; Aasa and

Vanngard, 1975). $n_{ij}(T)$ is the temperature-dependent population difference between the resonant states. The meanings of $Q(\theta - \theta_0)$ and $N(\theta_0, \sigma_\theta)$ are described in the next section. Experimentally the derivative of the absorption line, namely $\partial I(B) / \partial B$, has been measured. The resonant field position and other quantities in Eq. 1 are angular dependent. The simulation of EPR spectra of complex systems with $S > 1/2$ are extremely time-consuming because, in addition to averaging over all orientations of molecules according to Eq. 1, the integration over randomly distributed zero-field splitting parameters is needed. The positions of the resonant fields at each orientation are calculated precisely, using the general eigenvalue method (Belford et al., 1973). Once these fields are known the wavefunctions of the states and the other quantities needed in Eq. 1 are calculated by the usual methods (Belford et al., 1973; Wang and Hanson, 1996; Pilbrow, 1990). To reduce the amount of time required for simulation, an interpolation scheme has been applied. A restricted number of equally spaced directions of the external magnetic field (θ , ϕ) are chosen by the apple-peel method of partitioning of a unit sphere (van Veen, 1978; Gribnau et al., 1990). The one-dimensional cubic spline interpolation method (Bu-qing and Ding-yuan, 1989) has then been applied along both θ and ϕ angles. A method for tracking the angular dependence of the resonant field for each pair of levels has been implemented in a computer program and will be described separately. Additional integration over the rhombic ZFS parameter E , to which the EPR spectra of non-Kramers systems are particularly sensitive (Hendrich and Debrunner, 1989), has been achieved by numerical integration of Eq. 1 over E , assuming a Gaussian distribution to represent the spread of E (Hendrich and Debrunner, 1989).

Analysis for mosaic spread

The signals at $g = 6$ (high-spin ferric heme) and $g = 3$ (low-spin ferric heme) have well-known orientations with respect to the heme axes. The $g = 6$ contains the two g tensor components g_x and g_y , oriented in the heme plane along the Fe-N pyrrole axes of the porphyrin. $g = 3$, being g_z , lies along the heme normal. Therefore with perfect alignment of all of the protein molecules the two signals at $g = 6$ and $g = 3$ would be expected to drop to zero intensity at $\theta = 0^\circ$ and 90° , respectively. That this does not occur implies there is imperfect or incomplete orientation of the protein molecules. This phenomenon, known as mosaic spread, was analyzed in the seminal paper of Blum et al. (1978). We have analyzed mosaic spread with this approach by averaging the probability of the membrane orientation away from the true orientational angle θ_0 . This is modeled as a Gaussian distribution of the tilts of the normal to the

multilayer plane with half-width of σ_θ :

$$Q(\theta - \theta_0) = \exp\left(-\left(\frac{\theta - \theta_0}{\sigma_\theta}\right)^2\right)$$

The averaging is performed by numerical integration followed by division by the normalizing factor $N(\theta_0, \sigma_\theta) = 2\pi \int_0^\pi Q(\theta - \theta_0) \sin \theta d\theta$, which, in the case of irregular distribution, depends on the parameter σ_θ as well as on the specified angle θ_0 . For regular distribution along the unit sphere, as for molecules in solution, we can let $\sigma_\theta \rightarrow \infty$. $N(\theta_0, \sigma_\theta)$ then reduces to the well-known normalizing factor 4π . The dependence of the normalizing factor on the orientational angle θ_0 is an indication that areas on the unit sphere covered by various spreads of applied magnetic fields with an effective thickness σ_θ are different from one orientation to another. The need to use a normalization factor does not appear to have been appreciated in earlier work. Only after such an analysis can the orientation dependences of the broad signals at $g \approx 12$ and $g \approx 3$ regions be obtained and the results compared with a theoretical simulation. Calculations using both the $g = 6$ and $g = 3.0$ signals give similar values of 21° for this parameter σ_θ . This compares with values of 25° obtained for cytochrome *c* oxidase in membranes by Blum et al. (1978).

Energy level scheme

To account for the angular dependences of the parallel and perpendicular mode features we require an energy level scheme on which an assignment can be based. We therefore test the results against an energy level scheme that accounts well for other magnetic data, including the parallel and perpendicular mode EPR signals of cytochrome *bo*₃ in glassy solutions (Oganesyan et al., 1998). In this model the energy levels of two interacting metal ions are described by the following spin-Hamiltonian (Oganesyan et al., 1998):

$$\begin{aligned} \hat{H} = & [g\beta B\hat{S} + D(\hat{S}_z^2 - \hat{S}^2/3) + E(\hat{S}_x^2 - \hat{S}_y^2)]^{\text{Fe}} \\ & + [g\beta B\hat{S}]^{\text{Cu}} - \hat{S}_{\text{Fe}} \cdot \mathbf{J} \cdot \hat{S}_{\text{Cu}} \end{aligned} \quad (2)$$

The first term represents the Zeeman interaction and zero-field splittings (ZFS) at iron (D and E are the axial and rhombic ZFS parameters), the second term is the Zeeman interaction at Cu_B(II), and the third is the spin-coupling between the two metals defined by \mathbf{J} , the exchange coupling tensor. A basis set is constructed using products of the single ion spin functions $|S_1, M_1\rangle|S_2, M_2\rangle$, where S_1 and S_2 refer to the total spins of the individual ions.

For the case of high-spin Fe(III) and Cu(II), $S_1 = 5/2$ and $S_2 = 1/2$. In the limit of strong exchange coupling, $|\mathbf{J}| \gg |D|$, the 12 product functions split into two multiplets of total spin $S' = 2$ and $S' = 3$. For the case of $|\mathbf{J}| \ll |D|$, the weak coupling limit, using a D value at the Fe(III) heme of 5.0 cm^{-1} , the $S = 5/2$ levels of Fe(III) are split into three

Kramers pairs. The pair with effective spin $S = 1/2$ is 10 cm^{-1} ($2D$) below the next highest pair. An isotropic \mathbf{J} value of $\sim 1 \text{ cm}^{-1}$ will couple this pair with the $S = 1/2$ Kramers pair from Cu_B(II) to give four energy states (Eq. 3; see Fig. 6). In order of ascending energy, the effective spin components along the Fe-Cu axis are 0, +1, -1, 0:

$$\begin{aligned} |A\rangle &= \frac{1}{\sqrt{2}} \left(\left| \frac{1}{2}, \frac{-1}{2} \right\rangle - \left| \frac{-1}{2}, \frac{1}{2} \right\rangle \right) \quad M_s = 0 \\ |B\rangle &= -\sin \phi \left| \frac{3}{2}, \frac{-1}{2} \right\rangle + \cos \phi \left| \frac{1}{2}, \frac{1}{2} \right\rangle \quad M_s = +1 \\ |C\rangle &= -\sin \phi \left| \frac{-3}{2}, \frac{1}{2} \right\rangle + \cos \phi \left| \frac{-1}{2}, \frac{-1}{2} \right\rangle \quad M_s = -1 \\ |D\rangle &= \frac{1}{\sqrt{2}} \left(\left| \frac{1}{2}, \frac{-1}{2} \right\rangle + \left| \frac{-1}{2}, \frac{1}{2} \right\rangle \right) \quad M_s = 0 \end{aligned} \quad (3)$$

where $\tan 2\phi = \sqrt{8J}/(2D - J)$. $|B\rangle$ and $|C\rangle$ are axially degenerate except in the presence of a rhombic distortion, E , when they are split into two states: $|B'\rangle = 1/\sqrt{2}(|B\rangle - |C\rangle)$ and $|C'\rangle = 1/\sqrt{2}(|B\rangle + |C\rangle)$.

Anisotropy of the \mathbf{J} tensor (Eq. 2) is required to account satisfactorily both for the observed resonant field values and for the relative transition intensities in parallel and perpen-

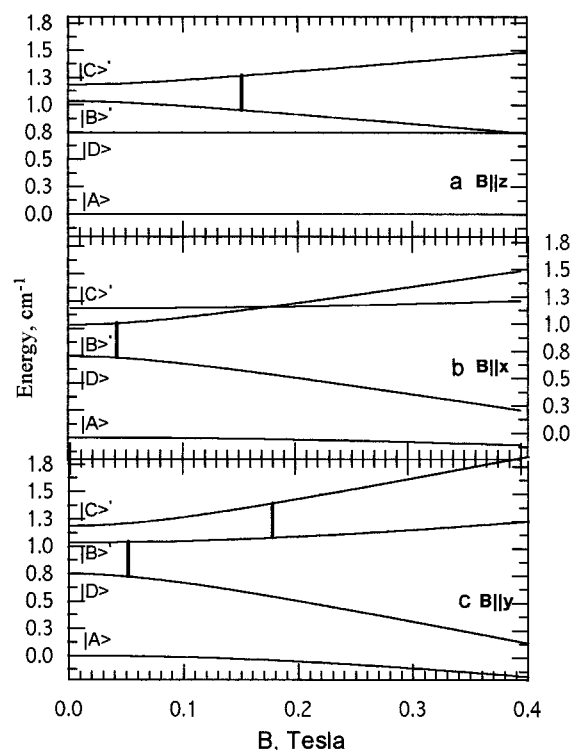


FIGURE 6 The four energy levels generated by exchange coupling of effective spins, $S = 1/2$, on high-spin Fe(III) heme and Cu_B(II), as described in the text, with a magnetic field applied along the three heme principal axes x , y , and z .

dicular modes. The resulting energy levels as a function of \mathbf{B}_{xyz} the magnetic field along each principal axis are shown in Fig. 6 for the weak coupling case. This scheme is used as the basis for the simulation of the angular dependences of $g' \approx 12$ features in the parallel and perpendicular mode EPR described in the next section.

Simulation of angular variation of EPR

Simulated angular variations of the EPR spectra in perpendicular and parallel modes in the regions of $g' \approx 12$ ($\mathbf{B} \approx 0.05\text{T}$) and $g \approx 6$ ($\mathbf{B} \approx 0.11\text{T}$) are shown in Figs. 7 and 8, respectively. The $g \approx 6$ signal has been simulated using the set of parameters that account for the frozen solution spectrum, namely, $D = 5\text{ cm}^{-1}$, $E = 0\text{ cm}^{-1}$, with linewidths $\Delta_{xyz} = [0.01\ 0.015\ 0.015]\text{ cm}^{-1}$. The $g \approx 6$ signal integrates to $\sim 7\%$ of uncoupled high-spin Fe(III) heme. The $g' \approx 12$ signal is simulated using the following parameters: $D = 5\text{ cm}^{-1}$, $E = 0.22\text{ cm}^{-1}$, with a Gaussian spread of E $\sigma_\theta = 0.05\text{ cm}^{-1}$ and with components of the coupling tensor (expressed in the heme coordinate frame) as $\mathbf{J}_{xyz} = [-0.25\ -0.25\ -1.55]\text{ cm}^{-1}$. The mosaic spread was estimated to be 21° , and for the $g' \approx 12$ signal α is 30° . Note that there is a contribution to the experimental spectra from minor components of unoriented fractions. Blum et al. (1978) also observed such contributions and estimated that $\sim 15\%$ of the EPR signal came from unoriented protein.

The angular dependences of the predicted resonant positions, expressed in the membrane coordinate system θ_0 between 0° and 90° and at selected values of ϕ equal to 0° , -60° , and -90° , for both the $g' \approx 12$ and $g \approx 6$ signals, are

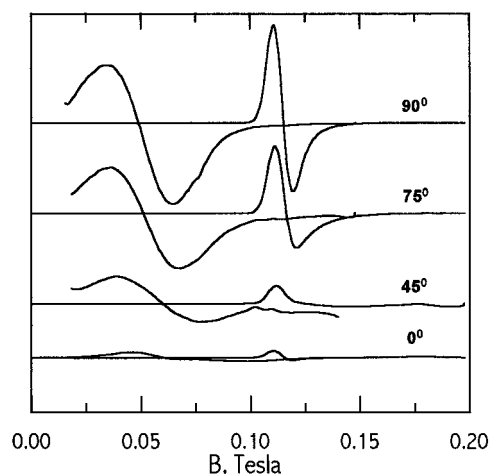


FIGURE 7 Simulated angular variations of perpendicular mode EPR spectra for $g \approx 12$ ($\mathbf{B} \approx 0.05\text{T}$) and $g \approx 6$ ($\mathbf{B} \approx 0.11\text{T}$) regions. $g \approx 6$ signal simulation parameters $D = 5\text{ cm}^{-1}$, $E = 0\text{ cm}^{-1}$, linewidths $\Delta_{xyz} = [0.01\ 0.015\ 0.015]\text{ cm}^{-1}$. $g \approx 12$ signal parameters: $D = 5\text{ cm}^{-1}$, $E = 0.22\text{ cm}^{-1}$, Gaussian spread of E $\sigma_\theta = 0.05\text{ cm}^{-1}$, $\mathbf{J}_{xyz} = [-0.25\ -0.25\ -1.55]\text{ cm}^{-1}$. The mosaic spread is estimated at 21° , and for the $g \approx 12$ signal α is 30° .

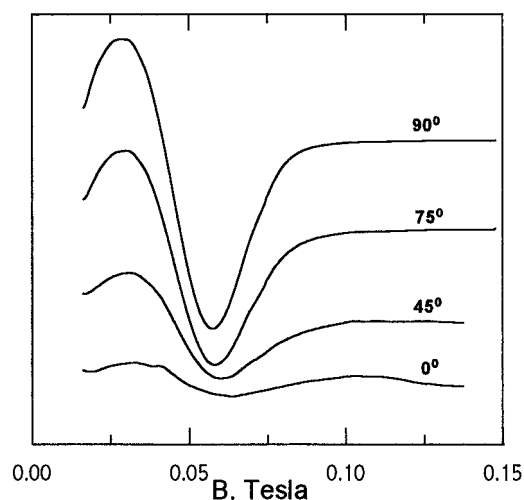


FIGURE 8 Simulated angular variations of the EPR spectra in parallel mode for $g \approx 12$. The spectra are generated from the same set of parameters as in Fig. 7.

shown in Fig. 9. Shaded regions indicate mosaic spread with $\sigma_\theta = 20^\circ$ at magnetic field orientations in the vicinity of $\theta_0 = 0$ and 90° , respectively. The importance of allowing for mosaic spread is apparent when we examine the origin of the angular variation of $g \approx 6$ signal. As can be seen from Fig. 9 *b*, without mosaic spread the signal would be isotropic at $\theta = 90^\circ$, because there is no dependence of the resonant field on ϕ . This would give a symmetrical derivative-shaped signal. However, asymmetrical $g \approx 6$ signals are observed. As the mosaic spread given by the factor σ_θ grows the anisotropy of the resonant position increases because the dependence on ϕ becomes more prominent (see the shaded area in Fig. 9 *b* near $\theta = 90^\circ$), resulting in asymmetrical shapes of both averaged absorption and derivative spectra. Hence the analysis of the form of $g \approx 6$ spectra at this orientation of magnetic field can serve as a rather sensitive measure of mosaic spread. Blum et al. (1978) used the $g = 3$ signal of low-spin heme to estimate the degree of mosaic spread. The most distinct effect on anisotropy is observed at $\theta = 0^\circ$, where a pronounced orientation dependence of \mathbf{B}_{res} is predicted by the shaded area near $\theta = 0^\circ$ (Fig. 9 *b*). The intensity is distributed over a wide range of fields, resulting in a spectral shape of low intensity with an almost Gaussian pattern centered at $\sim 0.11\text{T}$ (Fig. 7).

Because the angular dependence of the $g' \approx 12$ signal is closely similar to that of the $g \approx 6$, the same qualitative picture is expected for the angular variation as for the second signal. Indeed, at $\theta = 90^\circ$ orientation (Figs. 2 and 3 *a*), the $g' \approx 12$ signal in both parallel and perpendicular modes possesses the characteristic form of a broad asymmetrical derivative-shaped signal with a long negative-signed wing typical of oriented molecules and resulting from inhomogeneous broadening arising from the distribu-

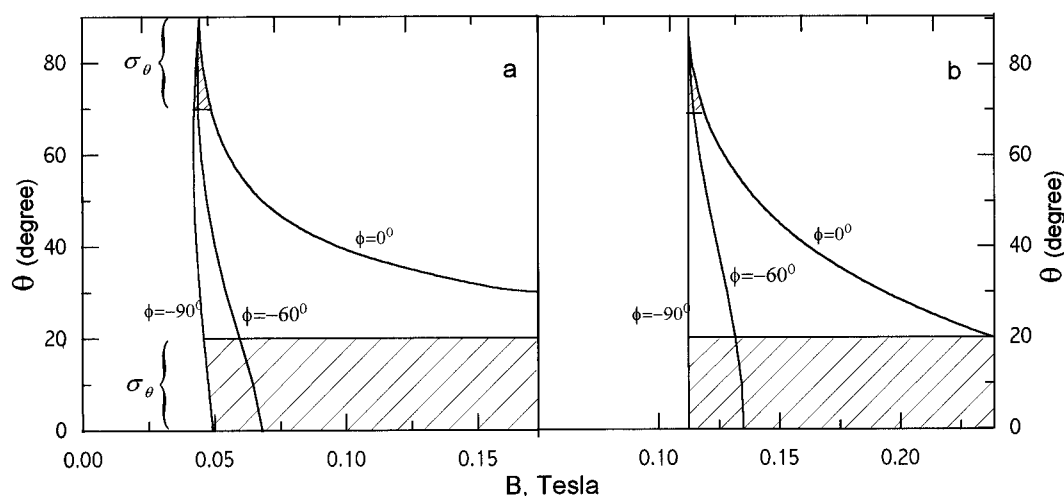


FIGURE 9 Angular dependencies of resonance positions of (a) $g \approx 12$ and (b) $g \approx 6$ signals expressed in a membrane coordinate system as a function of θ at selected values of ϕ of -0° , -60° , and -90° . The shaded region indicates the width of the mosaic spread with $\sigma_\theta = 21^\circ$ for magnetic field orientations relative to membrane plane in the vicinity of $\theta_0 = 0^\circ$ and 90° , respectively.

tion in, and averaging over, E alone (Hendrich and Debrunner, 1989; Abragam and Bleaney, 1970). As the applied magnetic field approaches the membrane plane, the signal at first becomes more symmetrical because of the compensating effects between, on one hand, inhomogeneous broadening from E distribution and, on the other, broadening due to an increasing angular anisotropy. Finally the signal loses all significant intensity, as shown in Figs. 1–3, *a* and *b*.

Assignment of EPR

The simulations show that the $g' \approx 12$ and $g' \approx 3.3$ signals are due to resonant transitions between states $|D\rangle$ and $|B'\rangle$ and between $|B'\rangle$ and $|C'\rangle$, respectively (Fig. 6). In principle, parallel mode signals can arise between any pair of states that have nonzero transition moments (Zeeman components) along the direction of the applied field. In this case, for example, when the magnetic field is applied along the heme principal axis z , intensity can appear for transitions between states $|B'\rangle$ and $|C'\rangle$, a so-called $\Delta M = \pm 2$ transition, or, when the field is applied along the principle axis x , between states $|D\rangle$ and $|B'\rangle$, a $\Delta M = \pm 1$ transition. Generally for orientations of the applied field along principal axes i the transition probability depends on Δ , where Δ is the energy difference between two states in zero field, as $\langle M(i) \rangle \approx (\Delta/h\nu)^2$. Hence signals at low fields have high intensity in parallel mode, because Δ is similar to $h\nu$, whereas at high field the signal intensity is lower because the value of Δ must tend to zero to satisfy the resonance condition $h\nu = \sqrt{\Delta^2 + (2g\beta B)^2}$.

In perpendicular mode the resonant intensity becomes significant only by field-induced mixing with the other states, as, for example, for the field orientation $\mathbf{B} \parallel y$ (Fig. 6 *c*). Test calculations with the model show that, once the

resonance at low field, the $g' \approx 12$ signal, is assigned to the transition from $|D\rangle$ to $|B'\rangle$ states, a second resonance around $\mathbf{B} \approx 0.2\text{T}$ will inevitably arise between $|B'\rangle$ and $|C'\rangle$, as seen in Fig. 6. However, the intensity of this second signal is expected to be vanishingly small in parallel mode because it lies at a higher field, which in turn requires Δ to be very small, as emphasized earlier.

The fact that the experimentally observed angular variation of the $g' \approx 12$ EPR signal (Figs. 1–4) is similar in parallel and perpendicular modes is of crucial importance to the assignment of transitions. When a magnetic field lies along the membrane normal, in the heme plane, with $\theta = 90^\circ$, the signal is at maximum in parallel as well as perpendicular modes, indicating that the Zeeman matrix element between the resonant states is in the xy plane. This can occur for states $|D\rangle$ and $|B'\rangle$, which have Zeeman matrix elements along the x and y axes and hence will yield maximum resonances in both modes when the field is in the xy plane (Fig. 6, *b* and *c*). As the field changes orientation into the membrane plane where $\theta = 0^\circ$, the resonance moves to a higher field, giving only highly anisotropic signals of low intensity, as seen in Figs. 1–4.

This interpretation rules out transitions between states $|B'\rangle$ and $|C'\rangle$ ($\Delta M = \pm 2$) as candidates for the $g' \approx 12$ signal because the nonzero Zeeman matrix element between these states lie along the z axis, not in the xy plane, where its value will be zero. Hence the maximum intensity of the signal in parallel mode is predicted to occur when the magnetic field is in the membrane plane, $\theta = 0^\circ$, contrary to the experimental evidence. Computer simulations support this conclusion.

The observed angular variation of the $g' \approx 12$ signal in parallel mode is also inconsistent with transitions within an $S = 2$ state arising from the so-called strong coupling

model. Earlier interpretations of the $g' \approx 12$ signal as arising from $\Delta M = \pm 4$ or ± 2 resonances either between $|\pm 2\rangle$ or $|\pm 1\rangle$ states of $S = 2$ (Hagen, 1982; Brudvig et al., 1986) are ruled out by these results because such resonances are predicted to have opposite angular dependences in parallel and perpendicular modes. It is possible within this strong coupling model to find resonant transitions between states $|0\rangle$ and $|+1\rangle$ or $|-1\rangle$ at $\mathbf{B} \approx 0.05\text{T}$ by using extremely low values for D of $\sim 0.2\text{ cm}^{-1}$. However, this results in the appearance of additional multiple resonances in both parallel and perpendicular modes, which have not been observed. Such a low value of D for high-spin Fe(III) heme is also inconsistent with a large body of experimental data on histidine coordinated hemes. Analysis of variable temperature and magnetic field circular dichroism (MCD) data of the high-spin heme in cytochrome *bo*₃ points unequivocally to more reasonable values for D of $\geq 5\text{ cm}^{-1}$ (Cheesman et al., manuscript in preparation).

The model predicts that the signal in the region of $g' = 3.3$ arises as a result of resonance between $|B'\rangle$ and $|C'\rangle$ states. In perpendicular mode the maximum intensity occurs when the magnetic field is in the membrane plane ($\theta = 0^\circ$) because, at this orientation, the angle between the y axis and the membrane plane is rather small ($\alpha \approx 30^\circ$), and the magnetic field is effectively in the vicinity of the yz heme plane, where the resonant field positions are restricted to a rather narrow interval near $\mathbf{B} \approx 0.2\text{T}$ (Fig. 6, *a* and *c*). As the field approaches the membrane normal ($\theta = 90^\circ$) it lies in the vicinity of the heme x axis, where the resonance disappears (Fig. 6 *b*). Hence the angular variation of signal $g' = 3.3$ tends to be opposite that observed for the $g' \approx 12$ signal. The experimental results shown in Figs. 1 and 2 suggest that the intensity in the region $g' \approx 3\text{--}4$ follows this prediction, but the signal-to-noise ratio is less than optimal, and further experiments are required at lower temperatures and higher microwave powers to improve the quality of the data.

DISCUSSION

The theoretical model presented by Oganessian et al. (1998) gave the first detailed description of a coupling scheme between high-spin Fe(II) heme and Cu(II) in which the D value at the heme was allowed to assume a value of $\sim 5\text{ cm}^{-1}$, as expected for a histidine coordinated high-spin heme, and the exchange coupling was found to be on the order of 1 cm^{-1} . The lowest energy levels in this case are a group of four arising from the coupling of two spins with effective $S = 1/2$, one on Cu(II) and the other from the lowest Kramers doublet of high-spin heme. The resulting energy levels have effective M_S values of 0, +1, -1, and 0. The separation of these levels in zero field depends on the values of D and E at the heme iron and the value of \mathbf{J} , the exchange coupling constant. It is necessary to use an anisotropic value of \mathbf{J} to obtain satisfactory fits to the data. The

perpendicular and parallel mode X-band EPR frozen solution spectra of the quinol oxidase cytochrome *bo*₃ were fitted satisfactorily with this weak coupling model, and proposals were made for the assignment of the transitions that give rise to the EPR features. The orientation-dependent data presented here provide a more stringent set of criteria against which this model and the proposed assignments can be tested. We have shown that the angular dependencies of the EPR signals in the $g' \approx 10\text{--}12$ region are correctly given by Oganessian (Oganessian et al., 1998). The orientation dependencies and the simulations for cytochrome *c* oxidase, however, require a modification to the assignment used in the earlier work. The transitions in the region of $g' \approx 12$ take place between $|D\rangle$ and $|B'\rangle$ when the field is in the heme xy plane. On the other hand, in fluoride-cytochrome *bo*₃ the spectra were simulated on the basis of assignments between $|B'\rangle$ and $|C'\rangle$ with the field in the yz plane. The energies of these four levels and the mixing of the levels depend sensitively on the choice of zero-field parameters and on the anisotropy of \mathbf{J} but not the overall magnitude of \mathbf{J} . Therefore it is possible that the assignments vary, as between the two enzymes.

Much experimental and theoretical effort has been expended to obtain an energy level scheme that will account for the magnetic properties of the binuclear center in cytochrome *c* oxidase, primarily with a view to arriving at an estimate of the magnitude and sign of the exchange coupling between the high-spin heme and the Cu_B (Hagen, 1982; Moss et al., 1978; Dunham et al., 1983). Previous work within a strong coupling model, in which the ground state separates into two distinct spin systems with $S = 2$ and $S = 3$, has assigned the transition at $g' = 12$ in cytochrome *c* oxidase to a $\Delta M = \pm 4$ transition within an $M = \pm 2$ non-Kramers pair of an $S' = 2$ system using a D value of 1.19 cm^{-1} in a Hamiltonian that assumes the strong coupling limit (Hagen, 1982). The relationship between D , the axial zero field splitting parameter of high-spin Fe(III) heme and D' is $D' \approx (4/3)D$ (Buluggiu, 1980). Hence the value of 0.9 cm^{-1} thus obtained for D is far too small for a high-spin Fe(III) heme with proximal histidine ligation, which is more typically $5\text{--}8\text{ cm}^{-1}$ (Brudvig et al., 1980). Using this value we were unable to simulate the essential spectral features observed in experiments on frozen solutions of protein, that is, the ratio of the peak intensities of the $g' \approx 12$ signal between the two modes and the appearance of the second signal ($g' \approx 3.2$) only in perpendicular mode. Moreover, the angular dependence results reported here are quite incompatible with a strong coupling model giving distinct spin systems with $S = 2$ and 3. In the strong coupling model the orientation dependences of transitions between $\Delta M_S = \pm 2$ and $\Delta M_S = \pm 4$ levels are predicted to be opposite in perpendicular and parallel modes, whereas the experimental results presented here show them to have the same orientation dependence. No previous attempts to assign the transition at $g' \approx 3.2$ have been made, although as shown in our

earlier work (Oganessian et al., 1998), this also severely restrains the model to a weak coupling.

Theoretical models based on both the strong and weak coupling limits have also been used to interpret Mössbauer and magnetic susceptibility data on cytochrome *c* oxidase (Moss et al., 1978; Dunham et al., 1983; Kent et al., 1983; Tweedle et al., 1978; Day et al., 1993; Barnes et al., 1991; Rusnak et al., 1987) as well as on heme-copper-bridged assemblies pertinent to cytochrome *c* oxidase (Kauffmann et al., 1997). Mössbauer spectra of the a_3 -Cu_B site of oxidized *Thermus thermophilus* c_1aa_3 could be simulated equally well in terms of a weak ($J \approx 1 \text{ cm}^{-1}$) or a strong ($J > 7 \text{ cm}^{-1}$) coupling (Rusnak et al., 1987). Both models could also fit the entire family of magnetization curves of the a_3 -Cu_B site of slow form of oxidized cytochrome *c* oxidase collected at several magnetic fields (Day et al., 1993). Thus in neither case could effective discrimination between the two models be obtained. Both studies invoked structural heterogeneity of the dinuclear site to account for the experimental data. The most complete fit of susceptibility magnetization curves for a sample of "slow" cytochrome *c* oxidase was obtained by Day et al. (1993), using the ZFS parameters: $S = 2$, $D = -7.4 \text{ cm}^{-1}$, $E/D = 0.27$. Because it is impossible to reconcile the $g' = 12$ EPR signal of the "slow" form with this set of parameters, the authors suggested that the signal may arise from a small subpopulation within the sample.

EPR signals from an unoriented non-Kramers ion at the X-band usually arise from only a fraction of the total spins because of the extreme anisotropy of the energy levels as a function of ZFS and magnetic field. Hence the calculation of average intensity differs from model to model, and quantitation of the number of spins contributing to the EPR spectrum cannot easily be obtained from a double integration procedure but instead requires spectral simulation (Hendrich and Debrunner, 1989). Our simulations (Oganessian et al., 1998) showed that the $g' = 12$ species arises from approximately the same number of spins as the signals from low-spin heme *a* ($S = 1/2$), which was in effect used as an internal standard. Hence the $g' = 12$ signal in our preparations of fluoride-cytochrome bo_3 does not arise from a minority component. Recent analyses of variable temperature and magnetic field MCD data also support this conclusion (Cheesman et al., manuscript in preparation).

The present work adds further experimental and theoretical weight to the case that the coupling between high-spin Fe(III) heme and the copper(II) ion pair at the active site of heme-copper oxidases is very weak in those species that give rise to the broad $g' = 12$ and $g' = 3.2$ signals. The results show clearly that the two metal ions are coupled with axially anisotropic $|J|$ values on the order of 1 cm^{-1} both in cytochrome *c* oxidase and in the quinol oxidase cytochrome bo_3 . Similar results have been obtained for the fast, formate and azide derivatives of cytochrome bo_3 (Oganessian et al., 1998). We shall shortly be reporting an analysis of the MCD

magnetization of high-spin heme a_3 in a coupled state with Cu_B(II) that leads to similar conclusions. Thus the broad signals in the low-field region that have been known for so long in the oxidase field are now understood in rather complete detail. This leads to the conclusion that the interaction is weak and the EPR spectrum is not greatly influenced by a ligand bound to either one of the two metal ions, provided that the heme remains high spin and that $J \ll D$. In this case the energy levels are dominated by D , the heme axial ZFS, and only secondarily influenced by the value of J . This contrasts with the situation in which cyanide ion is bound at the binuclear center (Thomson et al., 1982), switching the heme low spin and coupling the two spins ferromagnetically via the bridging cyanide ion. When other species occupy the site that could bridge between heme Fe(III) and Cu_B(II), such as peroxide, as recently proposed from the x-ray structural data (Yoshikawa et al., 1998), the strength of the coupling is not known. In the absence of the distinctive EPR spectra discussed in this paper, other diagnostic methods will need to be brought to bear.

We thank G. N. George for communicating his results of the angular dependence of the perpendicular mode EPR of oriented multilayers of bovine cytochrome *c* oxidase at the X- and Q-bands many years ago. These experimental results are consistent with our model.

This work was funded by the UK Biotechnology and Biological Sciences Research Council by grants GR/J33142 to WJI, BO1727 and BO2073 to AJT, and BO3032-1 to the Metalloprotein Center.

REFERENCES

- Aasa, R., and T. Vanngard. 1975. EPR signal intensity and powder shapes: a reexamination. *J. Mag. Res.* 19:308–315.
- Abraham, A., and B. Bleaney. 1970. *Electron Paramagnetic Resonance of Transition Ions*. Clarendon Press, Oxford.
- Barnes, Z. K., G. T. Babcock, and J. L. Dye. 1991. Magnetic state of the a_3 center of cytochrome *c* oxidase and some of its derivatives. *Biochemistry*. 30:7597–7603.
- Belford, G. G., R. L. Belford, and J. F. Burkhalter. 1973. Eigenfields: a practical direct calculation of resonance fields and intensities for field-swept fixed-frequency spectrometers. *J. Mag. Res.* 11:251–265.
- Blum, H., H. J. Harmon, J. J. Leigh, J. C. Salerno, and B. Chance. 1978. The orientation of a heme of cytochrome *c* oxidase in submitochondrial particles. *Biochim. Biophys. Acta*. 502:1–10.
- Brown, S., J. N. Rumbley, A. J. Moody, J. W. Thomas, R. B. Gennis, and P. R. Rich. 1994. Flash photolysis of the carbon monoxide compounds of wild-type and mutant variants of cytochrome *bo* from *Escherichia coli*. *Biochim. Biophys. Acta*. 1183:521–532.
- Brudvig, G. W., R. H. Morse, and S. I. Chan. 1986. A comparison of an exchanged-coupled Fe(III)-Cu(III) model with a Fe(IV) model for the O₂ binding site in oxidized cytochrome *c* oxidase via EPR spectral simulations. *J. Mag. Res.* 67:189–201.
- Brudvig, G. W., T. H. Stevens, and S. I. Chan. 1980. Reactions of nitric oxide with cytochrome *c* oxidase. *Biochemistry*. 19:5275–5285.
- Brudvig, G. W., T. H. Stevens, R. H. Morse, and S. I. Chan. 1981. Conformations of oxidized cytochrome *c* oxidase. *Biochemistry*. 20:3912–3921.
- Buluggiu, E. J. 1980. ESR aspects of the Mn²⁺-Cu²⁺ coupled pair. *J. Phys. Chem. Solids*. 41:43–45.

- Bu-qing, S., and L. Ding-yuan. 1989. Computational Geometry—Curves and Surface Modeling. Academic Press, San Diego.
- Calhoun, M. W., R. B. Gennis, W. J. Ingledew, and J. C. Salerno. 1994. Strong-field and integral spin-ligand complexes of the cytochrome *bo* quinol oxidase in *Escherichia coli* membrane preparations. *Biochim. Biophys. Acta*. 1206:143–154.
- Cheesman, M. R., N. J. Watmough, R. B. Gennis, C. Greenwood, and A. J. Thomson. 1994. Magnetic circular dichroism studies of *Escherichia coli* cytochrome *bo*. Identification of high-spin ferric, low-spin ferric and ferryl [Fe(IV)] forms of heme *o*. *Eur. J. Biochem.* 219:595–602.
- Chepuri, V., and R. B. Gennis. 1990. The use of gene fusions to determine the topology of all the subunits of the cytochrome *o* terminal oxidase complex of *Escherichia coli*. *J. Biol. Chem.* 265:12978–12986.
- Cooper, C. E., and J. C. Salerno. 1992. Characterization of a novel $g' = 2.95$ EPR signal from the binuclear center of mitochondrial cytochrome *c* oxidase. *J. Biol. Chem.* 267:280–285.
- Day, E. D., J. Peterson, M. S. Sendova, J. R. Schoonover, and G. Palmer. 1993. Magnetization of fast and slow oxidized cytochrome *c* oxidase. *Biochemistry*. 32:7855–7860.
- Dunham, W. R., R. H. Sands, R. E. Shaw, and H. Beinert. 1983. Multiple frequency EPR studies in three forms of oxidized cytochrome *c* oxidase. *Biochim. Biophys. Acta*. 748:73–85.
- Green, D. E., and D. M. Ziegler. 1963. Electron transport particles. *Methods Enzymol.* 6:416–424.
- Greenaway, F. T., S. H. P. Chan, and G. Vincow. 1977. An EPR study of the lineshape of copper in cytochrome *c* oxidase. *Biochim. Biophys. Acta*. 490:62–68.
- Gribnau, M. C. M., J. L. C. van Tits, and E. J. Reijerse. 1990. The efficient general algorithm for the simulation of magnetic resonance spectra of orientationally disordered solids. *J. Mag. Res.* 90:474–485.
- Hagen, W. R. 1982. EPR of non-kramers doublets in biological systems. Characterization of an $S = 2$ system in oxidized cytochrome *c* oxidase. *Biochim. Biophys. Acta*. 708:82–98.
- Hendrich, M. P., and P. G. Debrunner. 1989. Integer-spin electron paramagnetic resonance of iron proteins. *Biophys. J.* 56:489–506.
- Hosler, J. P., S. Ferguson-Miller, M. W. Calhoun, J. W. Thomas, J. J. Hill, L. J. Lemieux, J. Ma, C. Georgiou, J. Fetter, J. P. Shapleigh, M. M. J. Tecklenburg, G. T. Babcock, and R. B. Gennis. 1993. Insight into the active-site structure and function of cytochrome-oxidase by analysis of site-directed mutants of bacterial cytochrome-*aa₃* and cytochrome-*bo*. *J. Bioenerg. Biomembr.* 25:121–136.
- Hunter, D. J. B., A. J. Moody, P. R. Rich, and W. J. Ingledew. 1997. EPR spectroscopy of *Escherichia coli* cytochrome *bo* which lacks Cu_B. *FEBS Lett.* 412:43–47.
- Ingledew, W. J., J. Horrocks, and J. C. Salerno. 1993. Ligand binding to the haem-copper binuclear catalytic site of cytochrome *bo*, a respiratory quinol oxidase from *Escherichia coli*. *Eur. J. Biochem.* 212:657–664.
- Iwata, S., C. Ostermeier, B. Ludwig, and H. Michel. 1995. Structure at 2.8 Å resolution of cytochrome *c* oxidase from *Paracoccus denitrificans*. *Nature*. 376:660–669.
- Kauffmann, K. E., C. A. Goddard, Y. Zang, R. H. Holm, and E. Münck. 1997. Mössbauer and magnetization studies of heme-copper-bridged assemblies pertinent to cytochrome *c* oxidase. *Inorg. Chem.* 36:985–993.
- Kent, T. A., L. J. Young, G. Palmer, J. A. Fee, and E. J. Münck. 1983. Mössbauer study of beef heart cytochrome oxidase. *J. Biol. Chem.* 258:8543–8546.
- Lappalainen, P., and M. Saraste. 1994. The binuclear center of cytochrome oxidase. *Biochim. Biophys. Acta*. 1147:222–225.
- Little, R. H., M. R. Cheesman, A. J. Thomson, C. Greenwood, and N. J. Watmough. 1996. Cytochrome *bo* from *Escherichia coli*: binding of azide to Cu_B. *Biochemistry*. 35:13780–13787.
- Moss, T. H., E. Shapiro, T. E. King, H. Beinert, and C. Hartzell. 1978. Electronic state of heme in cytochrome oxidase III. The magnetic susceptibility of beef heart cytochrome oxidase and some of its derivatives from 7–200K. Direct evidence for an antiferromagnetically coupled Fe(III)/Cu(II) pair. *J. Biol. Chem.* 253:8065–8071.
- Oganesyan, V. S., C. S. Butler, N. J. Watmough, C. Greenwood, A. J. Thomson, and M. R. Cheesman. 1998. Nature of the coupling between the high-spin Fe(III) heme and Cu_B(II) in the active site of terminal oxidases: dual-mode EPR spectra of fluoride cytochrome *bo₃*. *J. Am. Chem. Soc.* 120:4232–4233.
- Pilbrow, J. R. 1990. Transition Ion Electron Paramagnetic Resonance. Oxford, Clarendon Press.
- Rusnak, F. M., E. Münck, C. I. Nitsche, B. H. Zimmerman, and J. A. Fee. 1987. Evidence for structural heterogeneities and a study of exchange coupling. Mössbauer studies of cytochrome *c₁aa₃* from *Thermus thermophilus*. *J. Biol. Chem.* 262:16328–16332.
- Salerno, J. C., and W. J. Ingledew. 1991. Orientation of the haems of the ubiquinol oxidase: O₂ reductase, cytochrome *bo* of *Escherichia coli*. *Eur. J. Biochem.* 198:789–792.
- Schoonover, J. R., and G. Palmer. 1990. Reaction of formate with the fast form of cytochrome oxidase: a model for the fast to slow conversion. *Biochemistry*. 30:7541–7550.
- Thomson, A. J., D. G. Eglinton, B. C. Hill, and C. Greenwood. 1982. The nature of heme *a₃* in the oxidized state of cytochrome *c* oxidase. Evidence from low temperature magnetic circular dichroism spectroscopy in near infra-red region. *Biochem. J.* 207:167–170.
- Tsukihara, T., H. Aoyama, E. Yamashita, T. Tomizaki, H. Yamaguchi, K. Shinzawa-Itoh, R. Nakashima, R. Yaono, and S. Yoshikawa. 1995. Structures of metal sites of oxidized bovine heart cytochrome *c* oxidase at 2.8 Å. *Science*. 269:1069–1074.
- Tsukihara, T., H. Aoyama, E. Yamashita, T. Tomizaki, H. Yamaguchi, K. Shinzawa-Itoh, R. Nakashima, R. Yaono, and S. Yoshikawa. 1996. The whole structure of the 13-subunit oxidized cytochrome *c* oxidase at 2.8 Å. *Science*. 272:1136–1144.
- Tweedle, M. F., L. J. Wilson, L. Garcia-Iniguez, G. T. Babcock, and G. Palmer. 1978. Electronic state of heme in cytochrome oxidase III. The magnetic susceptibility of beef heart cytochrome oxidase and some of its derivatives from 7–200K. Direct evidence for an antiferromagnetically coupled Fe(III)/Cu(II) pair. *J. Biol. Chem.* 253:8065–8071.
- van Veen, G. 1978. Simulation and analysis of EPR spectra of paramagnetic ions in powders. *J. Magn. Res.* 30:91–109.
- Wang, D., and G. R. Hanson. 1996. New methodologies for computer simulation of paramagnetic resonance spectra. *Appl. Magn. Reson.* 11: 401–415.
- Watmough, N. J., M. R. Cheesman, R. B. Gennis, C. Greenwood, and A. J. Thomson. 1993. Distinct forms of the haem *o*-Cu binuclear site of oxidized cytochrome *bo* from *Escherichia coli*. *FEBS Lett.* 319: 151–154.
- Yoshikawa, S., K. Shinzawa-Itoh, R. Nakashima, R. Yaono, E. Yamashita, N. Inoue, M. Yao, M. J. Tei, C. P. Libeu, T. Mizushima, H. Yamaguchi, T. Tomizaki, T. Tsukihara. 1998. Redox-coupled crystal structure changes in bovine cytochrome *c* oxidase. *Science*. 280:1723–1729.